18th International Conference on Structural Mechanics in Reactor Technology (SMiRT 18)
Beijing, China, August 7-12, 2005
SMiRT18-W101-9

THE RELATIONSHIP BETWEEN STRESSES AND DIMENSIONAL CHANGES IN NUCLEAR GRAPHITE MODERATOR BRICKS UNDER IRRADIATION

Haiyan Li*, Barry J. Marsden, Siu-Lun Fok
Nuclear Graphite Research Group
School of Mechanical, Aerospace and Civil Engineering
The University of Manchester
Manchester M60 1QD, U.K.
Tel: 44-(0)-161-275 4437
Fax: 44-(0)-161-275 4328
haiyan.li@manchester.ac.uk

ABSTRACT

A finite element stress analysis for a hypothetical nuclear graphite moderator brick has been carried out, considering dimensional and other property changes due to fast neutron irradiation. The stresses and deformations of the brick during operation and at shutdown have been examined. The results indicate a possible relationship between the turnarounds in the stresses and the dimensional change rate of the material. A theoretical solution is also presented for a hollow cylinder with similar dimensions, which is in good agreement with the finite element results for the graphite brick. Further analytical results are presented using different dimensional change rates. The results confirm that the turnaround in the hoop stress has a close relationship with the dimensional change rate of the material.

Keywords: Nuclear graphite, Moderator, Irradiation, Dimensional change, Stress

1 INTRODUCTION

A typical graphite moderated reactor core is constructed from a large number of graphite moderator bricks. Under fast neutron irradiation, graphite suffers damage to the crystal structure, which causes a change in its physical and mechanical properties, such as dimensional change and changes to Young's modulus, strength, coefficient of thermal expansion and thermal conductivity. In carbon dioxide cooled reactors, the graphite properties are also changed by the process of radiolytic oxidation, but this process is not considered in this paper.

Dimensional change is one of the important irradiation-induced changes to graphite. It is caused by the displacement of atoms from the crystal lattice into positions between the basal planes, resulting in 'c' axis growth and 'a' axis shrinkage as functions of fast neutron dose and irradiation temperature [1]. Under irradiation conditions of interest to modern graphite reactor designs, reactor graphite shrinks up to 'turnaround' and then expands with increasing fast neutron dose.

Linear dimensional changes of graphite, which can exceed 2% during service, can significantly influence the geometric sizes and internal stresses of the graphite bricks and, hence, the integrity of the whole reactor structure. Significant deformation or fracture of moderator bricks due to internal and external stresses may impair fuel and control rod movement [2]. Damage to the graphite components may also alter the coolant flow paths. Therefore, in graphite-moderated reactors, assessment of the integrity of graphite components is necessary to support operating safety cases.

Dimensional change data are obtained on graphite samples irradiated in material test reactors as a function of fast neutron dose and irradiation temperature [3], as are changes in other graphite material properties such as Young's modulus, strength, coefficient of thermal expansion (CTE), and irradiation creep, etc. In numerical calculation of nuclear graphite moderator bricks, dimensional change is considered to be an irradiation-induced strain that changes with irradiation temperature and irradiation dose.

The aim of this paper is to illustrate the relationship between the internal stresses of a hypothetical nuclear graphite moderator brick and the dimensional change property of the graphite material using both numerical and theoretical methods. The results can provide useful information to help reactor designers and operators to optimize new core designs and plan graphite monitoring campaigns.

2 NUMERICAL STRESS ANALYSIS FOR A NUCLEAR GRAPHITE BRICK

To investigate the effects of the dimensional change on the deformation and stresses in nuclear graphite bricks, calculations were carried out using the finite element method (FEM).

A standard finite element code ABAQUS [5] was used for the analysis; however, a user material subroutine (UMAT [5]) was required in order to describe the complex behaviour of graphite under high-temperature and irradiation conditions. In the development of the UMAT subroutine for graphite, material properties such as Young's modulus, dimensional change, coefficient of thermal expansion, and irradiation induced creep, were considered as functions of irradiation temperature and dose.

2.1 FE model

As the assessment was aimed at application to modern graphite-moderated reactor designs, isotropic graphite was assumed. Typical virgin properties are given in Table 1. Figures 1 and 2 give the dimensional change and its rate of change, while Figures 3 and 4 give the CTE and dynamic Young's modulus as functions of dose and temperature. Poisson's ratio was assumed to be 0.2 and independent of dose.

The geometry of the graphite brick analysed in this paper is shown in Figure 5. It is a rectangular block of 750mm high, with a square cross-section of 200mm×200mm and a circular bore of 100mm diameter. Applying symmetric conditions, only one eighth of the brick was selected for calculation. The finite element mesh is shown in Figure 6. Three-dimensional eight-node elements were used in this particular analysis.

For simplicity, the temperature was assumed to be uniform throughout the whole brick at 500°C and remain constant throughout reactor life. But the fast neutron dose was assumed to have a radial profile, i.e. decreasing with increasing radius. The end-of-life dose profile is shown in Figure 6. It was assumed that the dose increased linearly with time. The calculation simulated a period of 25 years operation with a shutdown every 2.5 years.

Table 1 Virgin graphite properties

Young's modulus (GPa)	10.0
Poisson's ratio	0.2
Coefficient of thermal expansion (10^{-6}/°C)	4.39

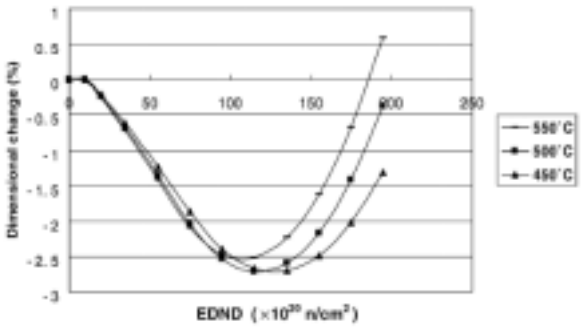

Fig. 1 Dimensional change vs. Dose

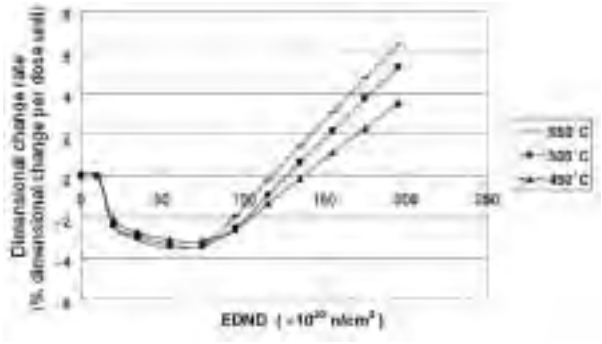

Fig. 2 Dimensional change rate vs. Dose

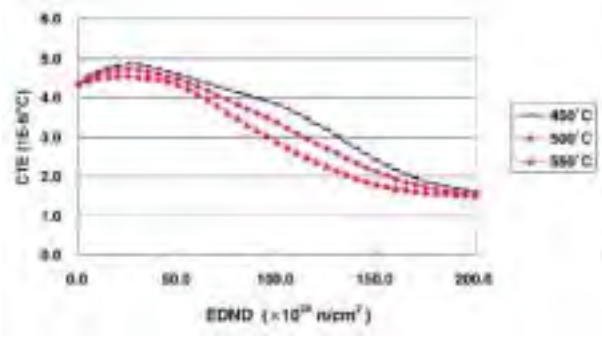

Fig. 3 CTE vs. Dose

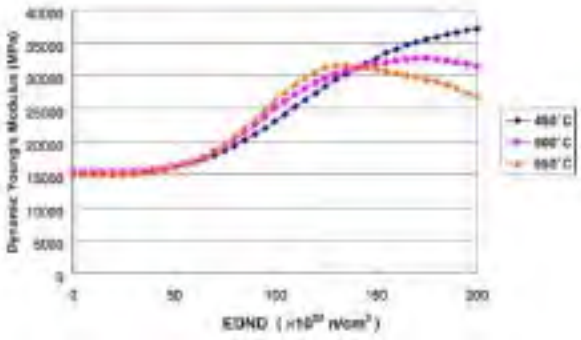

Fig. 4 Dynamic Young's modulus vs. Dose

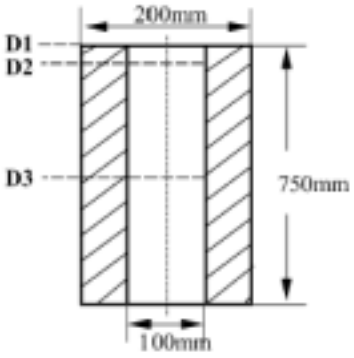

Fig. 5 Geometry of graphite brick

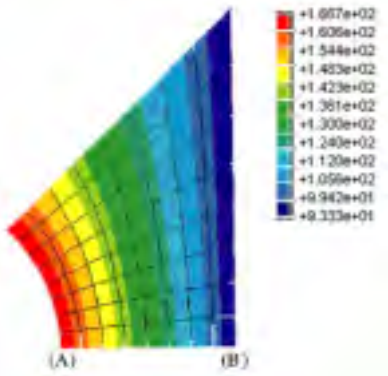

Fig. 6 FE mesh and dose profile

The irradiation creep rule used is [4]:

$$\varepsilon_{cr} = (1-\exp(-4\gamma))\frac{\sigma}{E_c} + 0.23\frac{\sigma}{E_c}\gamma \quad (1)$$

where ε_{cr} is the creep strain, E_c is the creep modulus as discussed in Reference [1], σ is the stress, and γ is the fast neutron dose (10^{20} n/cm^2 EDND).

2.2 FE results and discussion

Figure 7 shows the dimensional change rate against time at points A and B (see Figure 6) at mid-height of the brick. It can be seen that, due to the dose gradient, the dimensional change on the outside of the brick significantly lags the inside, leading to distortion of the brick shape and the generation of internal shrinkage stresses.

Figure 8 shows the exaggerated three-dimensional shapes of the brick at the 15th and 25th year of operation. Figure 9 shows the radial displacement at the bore (point A) along the axial distance at different times. It can be seen that turnaround occurs at the bore after about 22 years of operation for this particular brick shape. Figure 10 shows the radial displacement along the axial distance at different times on the outside of the brick (point B). The changes follow a similar trend to those at point A, but the radial displacement values are larger than those at the bore due to the greater radial distance. Before turnaround, the diameter at the end of the brick, D1 (shown in Figure 5), reduces more quickly than those at D2 and D3, resulting in a 'barrel' shape (Figure 8a). This is due to the fact that the end faces of the brick are in plane-stress condition while the interior is in plane-strain. The absence of an axial stress at the end faces allows greater radial displacements to occur there. For the same reason, after turnaround, the diameter at the end of brick, D1, increases more quickly than those at D2 and D3, thus resulting in a 'wheatsheaf' shape (Figure 8b). Furthermore, at height D2, where the transition from plane-stress

to plane-strain occurs, both the reduction before turnaround and the increase after turnaround are less than those at D1 and D3, resulting in a 'hump' just below the end face.

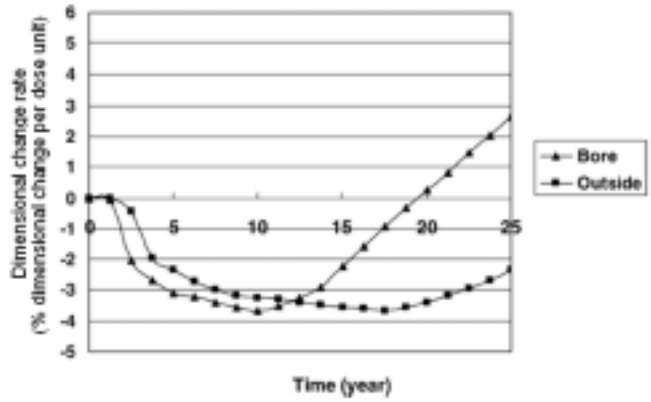

Fig. 7 Dimensional change rate vs. Time (at power)

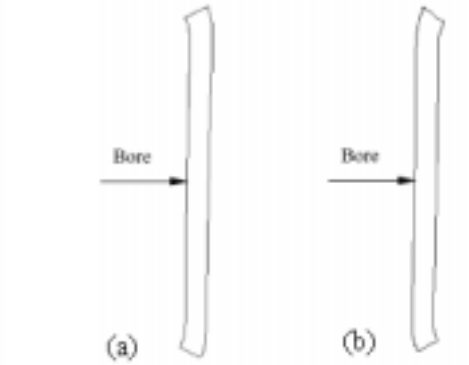

Fig. 8 Deformed shapes for the face of the brick exaggerated with a scale factor of 20: (a) time = 15 years; (b)time = 25 years

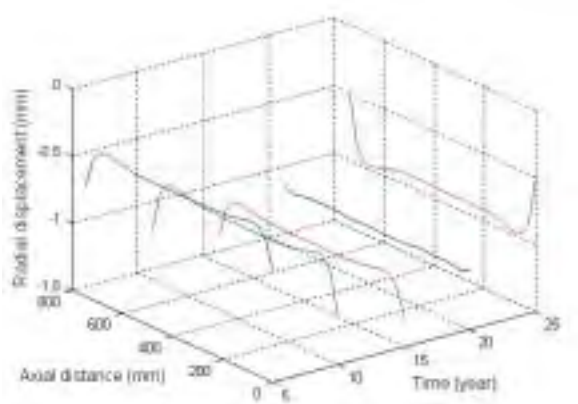

Fig. 9 Radial displacement vs. axial distance and time at the bore(at power).

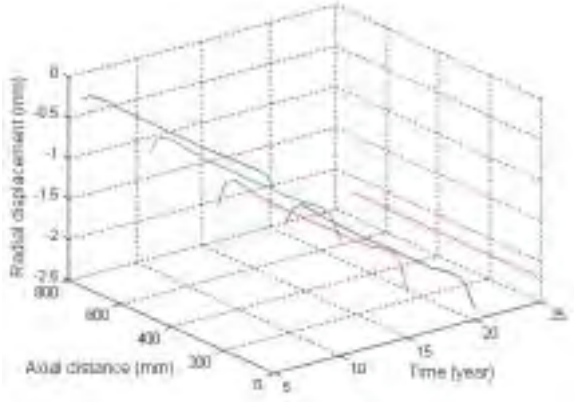

Fig. 10 Radial displacement vs. axial distance and time on the outer surface (at power).

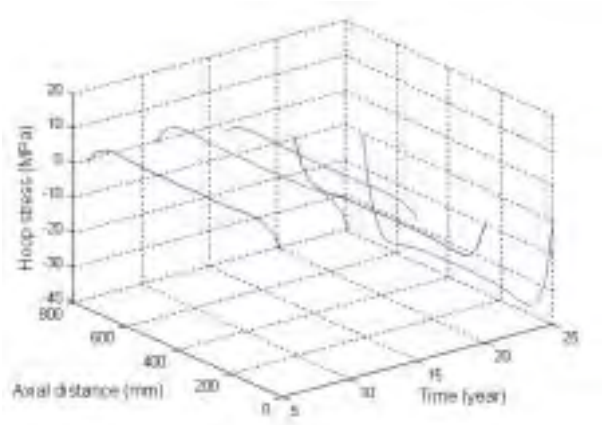

Fig. 11 Hoop stresses vs. axial distance and time at the bore (at power)

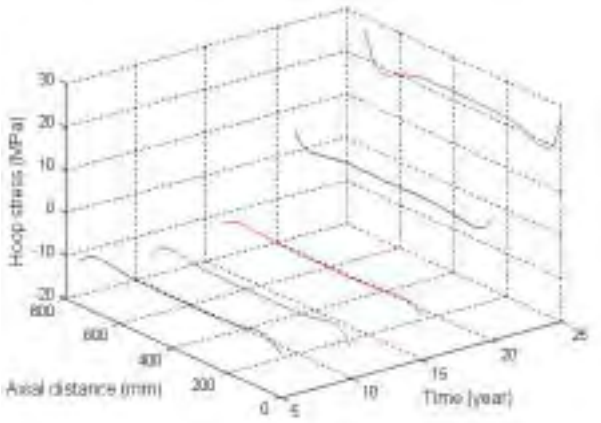

Fig. 12 Hoop stresses vs. axial distance and time on the outer surface (at power)

Figures 11 and 12 show the hoop stresses, at power, along the axial distance at different times at the bore and on the outer surface respectively. Figure 13 shows the hoop stress histories at power and at shutdown for both the inside and outside of the brick at different heights. It is clearly shown that the inside of the brick is

mainly in tension early in life and in compression later in life, and the outside is in compression early in life and in tension later in life. At shutdown, there is a significant increase in stress magnitude both on the inside and outside of the brick. The generation of the additional thermal stresses at shutdown is due to the fact that the irradiation induced changes to the coefficient of thermal expansion at the bore are different from those on the outside of the brick. Therefore, at shutdown, non-uniform thermal stresses arise as the temperature reduces.

Figure 14 shows the axial stress histories at power and at shutdown on both the inside and outside of the brick at different heights. It is worth noting that the axial stresses are of a similar magnitude to the hoop stresses.

By comparing Figures 7, 13 and 14, it can be seen that the turnaround of the hoop and axial stresses seems to occur at about the same time as that of the dimensional change rate at the bore, i.e. the 10th year of operation. This apparent relationship between the stresses and the dimensional change rate will be explored further in the theoretical analysis described below.

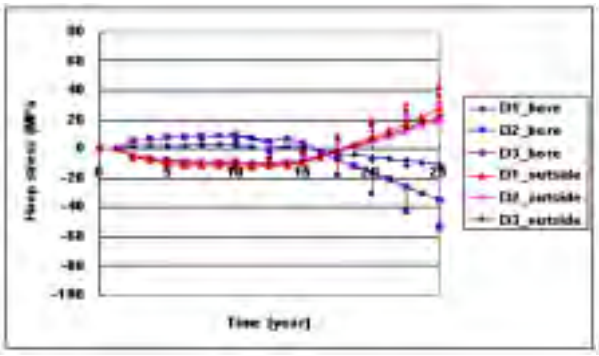

Fig. 13 Hoop stresses vs. time at different places (at power and shutdown).

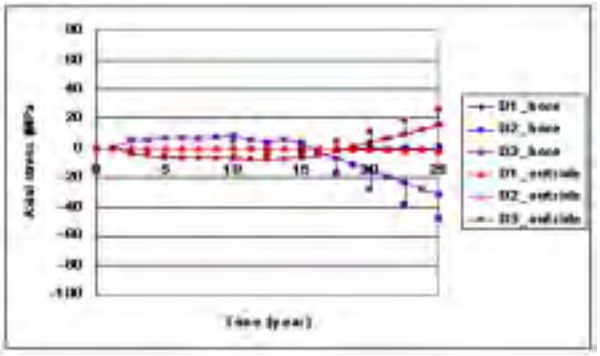

Fig. 14 Axial stresses vs. time at different places (at power and shutdown).

Note: see Figure 5 for positions of D1, D2 and D3.

3 THEORETICAL STRESS ANALYSIS

To verify the numerical solutions and to facilitate further sensitivity studies, a theoretical stress analysis was carried out on a simplified geometry. A graphite hollow cylinder with similar dimensions (i.e. 100mm ID and 200mm OD) as the graphite brick shown in Figure 5 was analyzed using the same material properties as those assumed in the FE analysis (Figures 1 to 4). The irradiation-induced dimensional change, creep and Young's modulus change were all considered. However, for simplification, only the secondary creep was considered.

3.1 Theoretical method [6]

Assuming axisymmetric and plane-stress conditions, we can write:

$$\varepsilon_\theta = \frac{1}{E}\left(\sigma_\theta - \nu\sigma_r\right) + \varepsilon_{dim} + \varepsilon_{c\theta} = \frac{u}{r} \tag{2}$$

$$\varepsilon_r = \frac{1}{E}\left(\sigma_r - \nu\sigma_\theta\right) + \varepsilon_{dim} + \varepsilon_{cr} = \frac{\partial u}{\partial r} \tag{3}$$

where $\boldsymbol{u}$ is the displacement in the radial ($\boldsymbol{r}$) direction; $\boldsymbol{E}$ is Young's modulus; ν is Poisson's ratio; $\boldsymbol{\varepsilon}_r$ and $\boldsymbol{\varepsilon}_\theta$ are the total radial and circumferential strains; $\boldsymbol{\sigma}_r$ and $\boldsymbol{\sigma}_\theta$ are the radial and circumferential stresses; $\boldsymbol{\varepsilon}_{dim}$ are the strains due to irradiation-induced dimensional change, which is the same in each direction for an isotropic graphite; and $\boldsymbol{\varepsilon}_{cr}$ and $\boldsymbol{\varepsilon}_{c\theta}$ are the radial and circumferential creep strains.

Ignoring primary creep, we can write

$$\varepsilon_{c\theta} = 0.23\int_0^\gamma \frac{\sigma_\theta - \nu\sigma_r}{E_c}\, d\gamma' \tag{4}$$

$$\varepsilon_{\mathbf{cr}} = 0.23\int_0^{\gamma}\frac{\sigma_{\mathbf{r}} - \nu\sigma_{\boldsymbol{\theta}}}{E_{\mathbf{c}}}d\gamma' \tag{5}$$

where E_c is the creep modulus and γ is the dose.

E, E_c, and ε_{dim} are approximated as fifth order polynomials of neutron dose γ:

$$\varepsilon_{dim} = A_0\gamma^5 + A_1\gamma^4 + A_2\gamma^3 + A_3\gamma^2 + A_4\gamma + A_5 \tag{6}$$

$$E = B_0\gamma^5 + B_1\gamma^4 + B_2\gamma^3 + B_3\gamma^2 + B_4\gamma + B_5 \tag{7}$$

$$E_{\mathbf{c}} = C_0\gamma^5 + C_1\gamma^4 + C_2\gamma^3 + C_3\gamma^2 + C_4\gamma + C_5 \tag{8}$$

The constants $A_0 - A_5$, $B_0 - B_5$ and $C_0 - C_5$ can be obtained by fitting the above polynomials to the material data curves such as those given in Figures 1 and 3.

The dose is assumed to vary with the radial distance (r) and time (t) as follows:

$$\gamma = (K_0 - K_1 r)t \tag{9}$$

where K_0 and K_1 are determined by the dose profile shown in Figure 6. Then, at a certain time t, E, E_c, and ε_{dim} can be expressed as functions of the radius r:

$$\varepsilon_{dim} = D_0 r^5 + D_1 r^4 + D_2 r^3 + D_3 r^2 + D_4 r + D_5 \tag{10}$$

$$E = E_0 r^5 + E_1 r^4 + E_2 r^3 + E_3 r^2 + E_4 r + E_5 \tag{11}$$

$$E_c = F_0 r^5 + F_1 r^4 + F_2 r^3 + F_3 r^2 + F_4 r + F_5 \tag{12}$$

with $D_0 - D_5$, $E_0 - E_5$ and $F_0 - F_5$ being functions of time t.

σ_r is usually much smaller than σ_θ and can therefore be ignored. Then, substituting (4) and (5) into (2) and (3) gives

$$\frac{1}{E}\sigma_{\boldsymbol{\theta}} + \varepsilon_{\mathbf{dim}} + 0.23\int_0^{\gamma}\frac{\sigma_{\boldsymbol{\theta}}}{E_{\mathbf{c}}}d\gamma' = \frac{u}{r} \tag{13}$$

$$\frac{1}{E}\left(-\nu\sigma_{\boldsymbol{\theta}}\right) + \varepsilon_{\mathbf{dim}} + 0.23\int_0^{\gamma}\frac{\left(-\nu\sigma_{\boldsymbol{\theta}}\right)}{E_{\mathbf{c}}}d\gamma' = \frac{\partial u}{\partial r} \tag{14}$$

These can be combined to give

$$\frac{\partial u}{\partial r} + \nu\frac{u}{r} = (1+\nu)\varepsilon_{dim} \tag{15}$$

Using (10), the displacement $\boldsymbol{u}$ can be solved, giving

$$u = \frac{G_0}{r^{\nu}} + \frac{D_0}{6+\nu}r^6 + \frac{D_1}{5+\nu}r^5 + \frac{D_2}{4+\nu}r^4 + \frac{D_3}{3+\nu}r^3 + \frac{D_4}{2+\nu}r^2 + \frac{D_5}{1+\nu}r \tag{16}$$

where G_0 is an unknown constant which can be determined, in the absence of external load, by the boundary condition

$$\int_{r_i}^{r_o} \sigma_\theta dr = 0 \tag{17}$$

σ_θ can be obtained from the differential equation resulting from substituting (16) into (13).

3.2 Theoretical results

Matlab 6.5, a powerful technical computing language software [7], was used to implement the theoretical analysis.

Figure 15 compares the theoretical hoop stress histories at the inner and outer surfaces of the cylinder with the corresponding FE results for the rectangular brick. It shows that the theoretical results are in good agreement with the FE results, especially in early life. The discrepancy can be attributed to the differences in geometries and the assumption of plane-stress or plane-strain condition. Therefore, the developed theoretical method can be used to approximate the stress change history for the graphite brick.

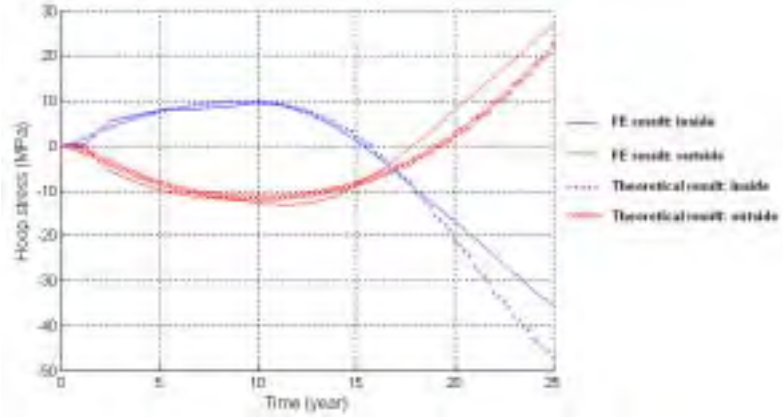

Fig. 15 Hoop stress histories at the bore and outer surface (at power)

To further examine the possible relationship between the turnarounds in the stresses and the dimensional change rate identified above, different hypothetical dimensional change curves were used in the theoretical analysis; see Figures 16 and 18.

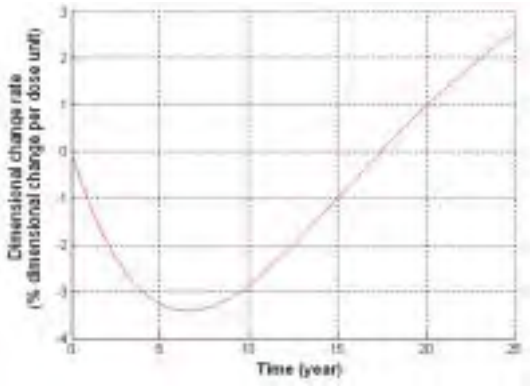

Fig. 16 Dimensional change rate vs.Time

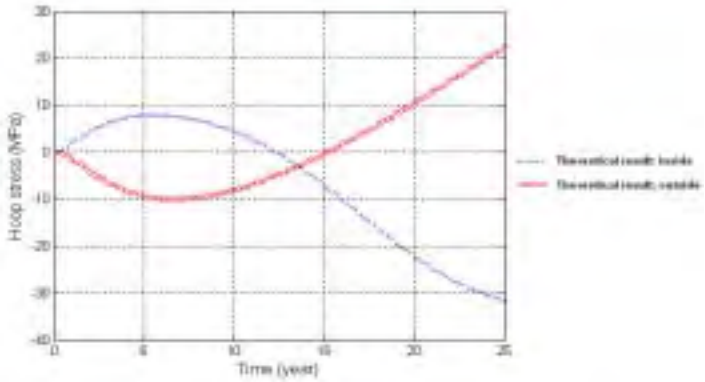

Fig. 17 Theoretical stress history at the bore and out surface

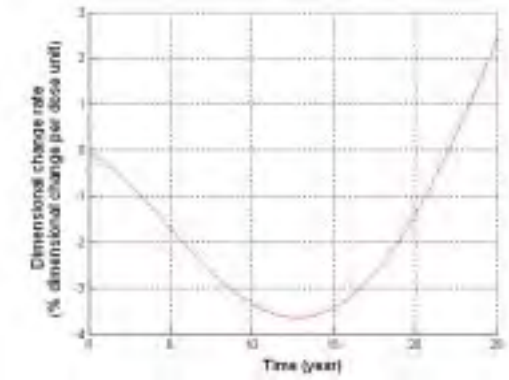

Fig. 18 Dimensional change rate vs.Time

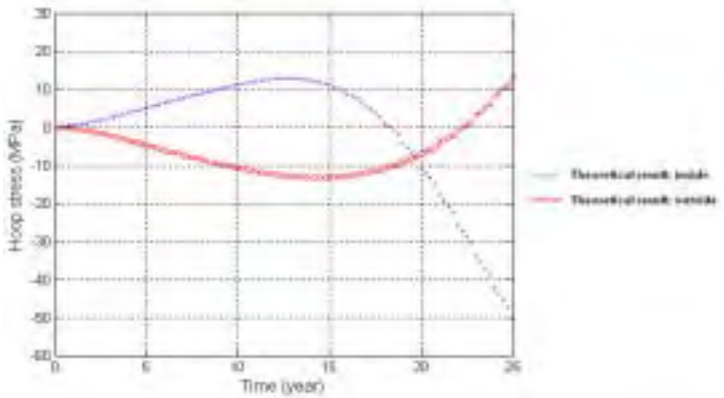

Fig. 19 Theoretical stress history at the bore and out surface

Figures 17 and 19 show the theoretical results obtained using the different dimensional change rate curves given in Figures 16 and 18. They confirm that the hoop stresses and the dimensional change rate are closely related: the turn-around of the hoop stresses take place at about the same time as that of the dimensional change rate.

4 CONCLUSIONS

From the above FE and theoretical stress analysis of a hypothetical nuclear graphite moderator brick, the following conclusions can be drawn:

- Stresses at the bore of the brick are tensile in the first half of life and compressive in the second half of life; while the opposite is true for stresses on the outer surface.
- The shape of the graphite brick changes from a barrel shape early in life to a wheatsheaf shape at the end of life.

- The axial stresses are of a similar order to the hoop stresses.
- The hoop stress history of the brick is closely related to the rate of irradiation-induced dimensional change of the graphite.
- The results from the theoretical analysis are in good agreement with the finite element results.
- The theoretical method can be used to predict the approximate stress history of nuclear graphite moderator bricks with a cylindrical geometry.

REFERENCE

[1] Marsden B.J. Graphite for High-Temperature Reactors. EPRI, Palo Alto, CA: 2001. 1003013.

[2] Curtis R.F., Jones S., Reed J., and Wickham A.J. The Development of Direct Core Monitoring in Nuclear Electric plc, Graphite Moderator Lifecycle Behaviour. IAEA-TECDOC-901, August 1996.

[3] Brocklehurst J.E. and Kelly B.T. Analysis of the Dimensional Changes and Structural Changes in Polycrystalline Graphite under Fast Neutron Irradiation. Carbon, 31(1993)155-178.

[4] Kelly B.T. and Brocklehurst J.E. UKAEA Reactor Group Studies of Irradiation-induced Creep in Graphite. Journal of Nuclear Materials, 65 (1977) 79-85.

[5] Hibbett, Karlson and Sorenson. ABAQUS Standard: version 6.1: user's manual. 2000.

[6] Cornwall W.S. Wigner Stresses. United Kingdom Atomic Energy Authority, TRG Report 40(R), 1962 (Available from the UK Public Records Office).

[7] Hanselman, Duane C. Mastering MATLAB 6. 2001.

